JLB

Brief Conclusive Report

Regulation of osteoclast structure and function by FAK family kinases

Brianne J. Ray, Keena Thomas,* Cynthia S. Huang,† Michael F. Gutknecht,* Edward A. Botchwey,† and Amy H. Bouton*,1*

*Department of Microbiology, Immunology, and Cancer Biology, University of Virginia, Charlottesville, Virginia, USA; and †The Wallace H. Coulter Department of Biomedical Engineering at Georgia Tech and Emory University, Atlanta, Georgia, USA

RECEIVED MAY 29, 2012; REVISED JULY 18, 2012; ACCEPTED AUGUST 14, 2012. DOI: 10.1189/jlb.0512259

ABSTRACT

Osteoclasts are highly specialized cells that resorb bone and contribute to bone remodeling. Diseases such as osteoporosis and osteolytic bone metastasis occur when osteoclast-mediated bone resorption takes place in the absence of concurrent bone synthesis. Considerable effort has been placed on identifying molecules that regulate the bone resorption activity of osteoclasts. To this end, we investigated unique and overlapping functions of members of the FAK family (FAK and Pyk2) in osteoclast functions. With the use of a conditional knockout mouse model, in which FAK is selectively targeted for deletion in osteoclast precursors ($FAK^{\Delta myeloid}$), we found that loss of FAK resulted in reduced bone resorption by osteoclasts in vitro, coincident with impaired signaling through the CSF-1R. However, bone architecture appeared normal in $FAK^{\Delta myeloid}$ mice, suggesting that Pyk2 might functionally compensate for reduced FAK levels in vivo. This was supported by data showing that podosome adhesion structures, which are essential for bone degradation, were significantly more impaired in osteoclasts when FAK and Pyk2 were reduced than when either molecule was depleted individually. We conclude that FAK contributes to cytokine signaling and bone resorption in osteoclasts and partially compensates for the absence of Pyk2 to maintain proper adhesion structures in these cells. *J. Leukoc. Biol.* 92: 1021–1028; 2012.

Introduction

Healthy bones undergo continuous remodeling as a result of the opposing activities of bone-forming osteoblasts and bone-resorbing osteoclasts. The risk of pathological disease is increased significantly when these actions become unbalanced, resulting in clinical disorders such as osteoporosis, Paget's disease, and metastatic bone disease. Bone metastatic disease has proven to be particularly difficult to treat and is usually considered a terminal illness [1]. Small molecule inhibitors targeting tyrosine kinases, such as c-Src (referred to as Src) and FAK/Pyk2, are being investigated in preclinical studies and clinical trials as treatments for bone metastatic disease [2, 3]. Whereas the function of Src and Pyk2 has been studied extensively in osteoclasts, FAK has been largely understudied in these cells.

Osteoclasts are highly specialized bone-resorbing cells that differentiate from circulating precursors originating in the bone marrow. Once osteoclast precursors arrive in the bone microenvironment, they receive differentiation signals, fuse to form large multinucleated cells, and begin to resorb bone [4]. M-CSF and RANKL are essential for osteoclast differentiation [5]. M-CSF also promotes osteoclast survival, spreading, motility, and enhancement of RANKL-mediated bone resorption [6–9]. Once osteoclasts mature and adhere firmly to bone, they rely on coordinated cytokine- and adhesion-mediated signaling to promote maximal bone resorption. The PTKs Src and Pyk2 are activated downstream of integrins and cytokine receptors during the process of bone degradation [10–13]. Mice harboring global genetic knockouts of Src or Pyk2 exhibit similar osteopetrotic phenotypes, underscoring the key role played by these kinases in bone homeostasis [14, 15]. Because of the close functional and structural relationship between FAK and these other tyrosine kinases, we hypothesized that FAK might function in similar signaling pathways to control bone resorption [16].

Podosome adhesions form in osteoclasts and mediate efficient bone resorption. These actin-rich adhesions promote attachment to bone and facilitate migration during the resorption cycle. Podosomes are composed of a dense actin core surrounded by actin-regulating proteins, adhesion molecules, adapter molecules, and tyrosine kinases [17–19]. As osteoclasts mature and begin to resorb bone, individual podosomes orga-

Abbreviations: $^{-/-}$=deficient, BV=bone volume, BV/TV=bone volume measured against total volume, CT=comparative threshold, $FAK^{\Delta myeloid}$=mice conditionally deleted for FAK in myeloid lineage cells, HA=hydroxyapatite, microCT=micro-computed tomography, pOC=preosteoclast, Pyk2=proline-rich tyrosine kinase 2, Tb.N=trabecular number, Tb.Sp=trabecular spacing, Tb.Th=trabecular thickness, TRAP=tartrate-resistant alkaline phosphatase, TV=total volume, VOI=volume of interest

The online version of this paper, found at www.jleukbio.org, includes supplemental information.

1. Correspondence: University of Virginia School of Medicine, 1340 Jefferson Park Ave., Charlottesville, VA 22908, USA. E-mail: ahb8y@virginia.edu

nize into higher-order clusters, rings, and belts [20, 21]. Src and to a lesser extent, Pyk2 regulate podosome dynamics and organization by influencing actin flux, podosome lifespan, and patterning [15, 22]. The absence of intact podosome belts in $Src^{-/-}$ and $Pyk2^{-/-}$ osteoclasts correlates with reduced bone resorption and impaired osteoclast function.

FAK and Pyk2 are the only members of the FAK family of nonreceptor PTKs [23–25]. In contrast to many other cell types, cells of the myeloid lineage, including osteoclasts, express both FAK and Pyk2. We have made use of a mouse model $FAK^{\Delta myeloid}$ to investigate the role of FAK in osteoclasts. Whereas we saw no abnormalities in BV or bone density in these mice, $FAK^{-/-}$ primary osteoclasts exhibited impaired bone degradation activity in vitro. This coincided with a significant reduction in Erk activation following M-CSF stimulation. In contrast to $Pyk2^{-/-}$ osteoclasts, $FAK^{-/-}$ cells were capable of forming higher-order podosome structures, including belts. However, depletion of FAK in a $Pyk2^{-/-}$ background exacerbated the podosome belt defect observed in $Pyk2^{-/-}$ osteoclasts, suggesting that FAK partially compensates for Pyk2 in regulating podosome structures. We conclude from these findings that FAK contributes to cytokine signaling and bone resorption in osteoclasts and partially compensates for the absence of Pyk2 to maintain proper adhesion structures and bone homeostasis in the bone microenvironment.

MATERIALS AND METHODS

Generation and genotyping of myeloid-specific FAK knockout mice

$FAK^{\Delta myeloid}$ mice were described previously [26]. $Pyk2^{-/-}$ mice were kindly provided by Dr. Brian R. Bond (Pfizer, St. Louis, MO, USA) [27], and the $FAK^{\Delta myeloid}/Pyk2^{-/-}$ mice were generated through genetic crosses. Animals were genotyped by PCR on tail DNA. FAK primers have been described previously [26]. Pyk2 primers are as follows: XREV1, 5′-CCT GCT GGC AGC CTA ACC ACA T-3′; WTF2, 5′-GGA GGT CTA TGA AGG TGT CTA CAC GAA C-3′; MUTF1, 5′-GCC AGC TCA TTC CTC CCA CTC AT-3′. Animals were handled in accordance with the guidelines the University of Virginia Animal Care and Use Committee (Charlottesville, VA, USA).

Antibodies and reagents

FAK, Pyk2, and Erk1/2 antibodies were described previously [26]. Src (2–17) mAb was provided by Dr. Sarah Parsons (University of Virginia). Cortactin 4F11 was obtained from Millipore (Billerica, MA, USA); AKT and phospho-AKT antibodies from Cell Signaling Technology (Danvers, MA, USA); α-mouse IgG Infrared Dye 800 from Rockland (Gilbertsville, PA, USA); α-rabbit IgG Alexa 680 from Molecular Probes (Grand Island, NY, USA); murine M-CSF and RANKL from PeproTech (Rocky Hill, NJ, USA); and the leukocyte acid phosphatase kit (TRAP staining) from Sigma-Aldrich (St. Louis, MO, USA).

Preparation and in vitro analysis of osteoclasts

Whole bone marrow was flushed from the tibiae and femurs of 6- to 10-week-old mice using ice-cold, serum-free α-MEM. Cells were pelleted; resuspended in α-MEM, supplemented with 10% FBS, 1% penicillin/streptomycin, and 5 ng/mL M-CSF; and plated overnight on plastic petri dishes. The next day, nonadherent cells were replated in complete α-MEM containing M-CSF (10 ng/nL) and RANKL (50 ng/mL) to induce osteoclast differentiation. pOCs were detected after 3 days and mature osteoclasts, after 6 days, as determined by TRAP staining.

To generate M-CSF-dependent macrophage-derived osteoclasts, whole bone marrow was collected as described above, plated for 3 days in 100 ng/mL M-CSF, and then replated in the presence of 100 ng/mL M-CSF and 100 ng/mL RANKL to induce osteoclast differentiation. To measure osteoclast spread area, 10–15 multinucleated cells from three or more random fields were traced using ImageJ software (NIH, Bethesda, MD, USA).

For M-CSF stimulation, Day 3 pOCs were plated at a density of 2×10^6 cells/well in a 12-well dish. Media and cytokines were refreshed every other day. After the appearance of multinucleated cells (5 or 6 days), the cultures were serum- and cytokine-starved for 2 h and then stimulated with M-CSF (30 ng/mL) for 5 and 15 min. Lysates were collected and subjected to immunoblot analysis as described previously [26]. Densitometry was performed using a LI-COR Odyssey infrared imaging system (LI-COR Biosciences, Lincoln, NE, USA) and densitometry values calculated based on Erk loading controls.

RT-PCR

RNA was collected from cultured cells using a Qiagen RNeasy mini kit (Valencia, CA, USA). cDNA was prepared by reverse transcription from 10 ng total RNA using random hexamers (1 μg) in a final reaction volume of 20 μl containing 200 U Superscript (Invitrogen Life Technologies, Carlsbad, CA, USA). TaqMan gene expression assay primers for PCR were purchased from Applied Biosystems (Carlsbad, CA, USA): FAK (Mm00433209_m1); Pyk2 (Mm00552827_m1); Src (Mm00436785_m1); and 18S rRNA (Mm03928990_g1). The PCR reaction was performed in triplicate using 10% of the volume of the first-strand synthesis in a TV of 25 μl that included 12.5 μl TaqMan Universal Mix and 250 nM final concentration of primers. cDNAs were subsequently quantified by real-time PCR using an ABI PRISM SDS7000 sequence detection system (Applied Biosystems). Thermocycling conditions were as follows: (1) 50°C for 2 min; (2) 95°C for 10 min; (3) 95°C for 15 s (denaturation); and (4) 60°C for 1 min (anneal/extend) for 40 cycles. The TaqMan primer-probe set for 18S rRNA with the Vic/Tamra detection system was used to measure 18S rRNA simultaneously in replicate samples. The ΔCT ($2^{-\Delta CT}$) method was used to quantify relative mRNA levels for the transcripts as described in User Bulletin #2 (Applied Biosystems) using18S rRNA as the reference and internal standard.

MicroCT imaging

The left tibiae of 10-week female mice were imaged using a quantitative microCT vivaCT40 scanner (Scanco Medical, Brüttisellen, Switzerland) with the following parameters: 10.5 μm voxel size, 55 kVp, 145 μA, high resolution, 21.5 mm diameter field of view, and 200 ms integration time. Bones were scanned in the same position and orientation with a specialized mouse tibia holder. The region of interest was set to include 100 slices of only trabecular bone distal to the proximal tibial growth plate,with automatic contouring excluding cortical bone density. Bone was thresholded at 501.3–2000 mg HA/cm^3. Morphometric parameters, including BV, Tb.N (mm^{-1}), Tb.Th (μm), and Tb.Sp (μm), were computed with Scanco Medical software. Three-dimensional volume renderings were performed with OsiriX 3.9 (Pixmeo, Geneva, Switzerland) from DICOM files. OsiriX images were thresholded and colored appropriately with the 16-bit color look-up table.

In vitro bone resorption assay

Day 3 (2.5×10^6) pOCs were plated on Becton Dickinson BioCoat Osteologic discs (Franklin Lakes, NJ, USA) in a 12-well dish, and the media were refreshed every other day. After 6 days, cells were removed by bleaching and the bone discs mounted on coverslips. Resorption pit area was measured using ImageJ software, where pits were traced in three random fields at a magnification of 10×.

Immunofluorescence

pOCs were seeded onto glass coverslips and fixed and stained 6–7 days later as described previously [26].

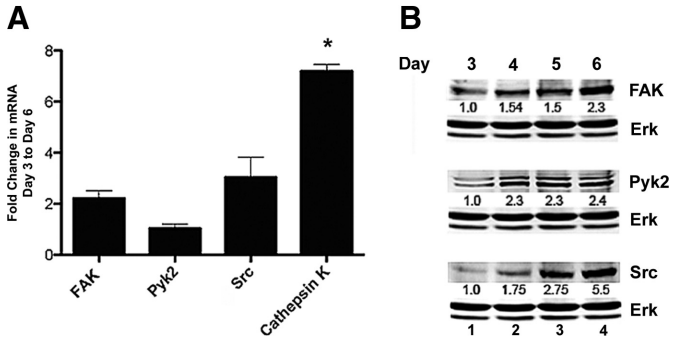

Figure 1. FAK, Pyk2, and Src are coordinately up-regulated during osteoclast differentiation. WT bone marrow cells were differentiated for 6 days in medium containing 10 ng/mL M-CSF and 50 ng/mL RANKL. (A) RNA was collected and subjected to quantitative RT-PCR. 18S rRNA was used as the internal standard. Fold-change from Day 3 to Day 6 was determined by dividing the Day 6 by Day 3 CT values ($2^{-\Delta CT}$); $n = 3$; $^*P < 0.05$. (B) Lysates were collected on Days 3–6 of differentiation and probed for FAK, Pyk2, Src, and Erk as a loading control. Immunoblots representative of three experiments are shown. The numbers below the FAK, Pyk2, and Src immunoblots indicate the fold-increase in expression relative to Day 3.

Statistical analysis

Podosome and microCT analysis results are presented as mean ± SEM. These statistical analyses were performed using a one-way general linear ANOVA, followed by Tukey's test for pairwise comparisons with Minitab 16 (Minitab, State College, PA, USA) at $P < 0.05$ significance. For all other statistical analyses, a two-tailed Student's t test assuming unequal variances was used to determine significance between condition means with a significance level of $P < 0.05$.

RESULTS AND DISCUSSION

FAK, Pyk2, and Src expression is coordinately up-regulated during osteoclastogenesis

Osteoclasts are derived from CD11b+ myeloid progenitor cells that reside in the bone marrow [28]. Interestingly, whereas these progenitors have no detectable FAK and very low levels of Pyk2 (Supplemental Fig. 1) [29, 30], mature osteoclasts express both of these molecules (**Fig. 1**) [31, 32]. To investigate changes in FAK and Pyk2 expression during osteoclastogenesis, mRNA levels were measured in primary bone marrow cells that were treated with M-CSF and RANKL for 3 days (pOCs) and 6 days (bona fide osteoclasts; Fig. 1A). Steady-state levels of cathepsin K mRNA increased over this time period, confirming that an established marker of osteoclast differentiation was up-regulated under these conditions [33]. By Day 6, >95% of the cells expressed the osteoclast marker TRAP (see Fig. 3A), indicating that the majority of cells had undergone osteoclastogenesis. Steady-state levels of FAK mRNA increased twofold between Days 3 and 6 of treatment, whereas Pyk2 mRNA levels remained constant (Fig. 1A). However, both FAK and Pyk2 protein expression increased during this differentiation process (Fig. 1B). Src mRNA and protein were similarly up-regulated, confirming earlier reports showing that Src levels increase during osteoclast differentiation [34, 35]. Interestingly, increased expression of FAK and Pyk2 during differentiation is not confined to osteoclasts, as a similar up-regulation has been reported in other hematopoietic cell lineages. For example, Pyk2 mRNA and protein expression increases during PMA-induced monocyte-to-macrophage differentiation of NB4 leukemia cells [36]. Similarly, FAK expression was shown to increase when bone marrow cells were cultured in the presence of GM-CSF [30]. The fact that these proteins are minimally expressed in myeloid progenitor cells and become significantly up-regulated during differentiation suggests that they play an important role in osteoclast function.

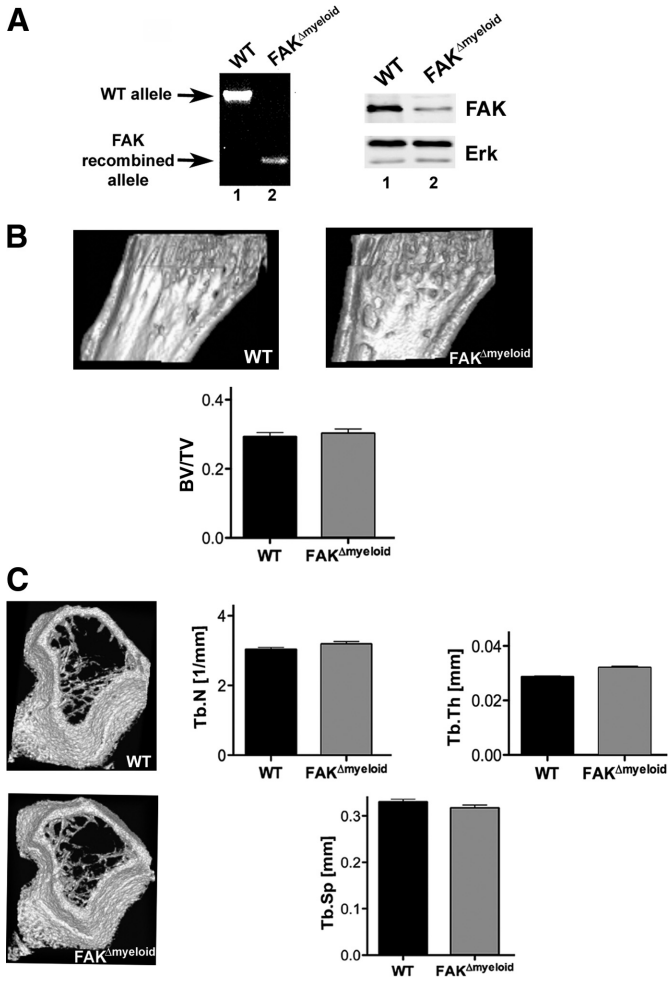

Figure 2. Conditional knockout of FAK in bone marrow-derived osteoclasts does not significantly alter bone phenotype in vivo. (A) Evidence for recombination of $FAK^{fl/fl}$ alleles in $FAK^{\Delta myeloid}$ osteoclasts. DNA was isolated from WT and in $FAK^{\Delta myeloid}$ osteoclasts, subjected to PCR, and separated by gel electrophoresis (left panels). FAK protein was isolated from these cells and detected by immunoblot, as described in Fig. 1 (right panels). (B) Representative images of bone cross-sections showing the VOI used for total BV analysis as described in Materials and Methods (upper images). Total BV/TV (mg HA/cm^3) in the VOI was computed with Scanco Medical software (lower panel). (C) Representative images of trabecular bone analyzed (left panels). The measurements of Th.N, Tb.Th, and Tb.Sp were computed with Scanco Medical software using a direct evaluation of the region of interest (graphs); $n = 3$/group.

Bone architecture in FAK$^{\Delta myeloid}$ mice appears normal despite the fact that FAK-depleted osteoclasts exhibit impaired bone resorption in vitro

Global loss of FAK results in embryonic lethality [37]. To study the role of FAK in osteoclasts, we took advantage of a conditional FAK knockout mouse in which Cre recombinase is expressed under the transcriptional control of the myeloid-specific lysozyme M promoter (FAK$^{\Delta myeloid}$) [26]. In this model, *FAK$^{fl/fl}$* alleles are targeted for deletion in cells of the myeloid lineage, including osteoclasts, macrophages, and neutrophils [26, 38]. FAK$^{\Delta myeloid}$ mice are viable and reproduce normally [26]. Recombination of the *FAK$^{fl/fl}$* allele in osteoclasts generated from FAK$^{\Delta myeloid}$ mice was confirmed by PCR and decreased FAK protein expression by immunoblot (**Fig. 2A**). Pyk2 expression remained largely unchanged under conditions of FAK depletion (see Fig. 5A, lanes 1 and 2).

Bone resorption by osteoclasts is a tightly regulated process that is essential for maintaining skeletal homeostasis. Defects in osteoclast function, coincident with an osteopetrotic phenotype, have been reported previously in global Src$^{-/-}$ and Pyk2$^{-/-}$ knockout mice [14, 15]. To determine whether this was also the case for FAK$^{\Delta myeloid}$ mice, we first assessed BV and trabecular bone architecture by microCT scanning of 10-week-old female mice. The high-resolution scans of the left tibia yielded a 3D model from which the cortical and trabecular BV/TV ratios were measured (Fig. 2B). BV/TV was similar between WT and FAK$^{\Delta myeloid}$ mice. These scans also allowed determination of three parameters of trabecular architecture: Tb.N, Tb.Th, and Tb.Sp (Fig. 2C). In all measures, the trabeculae of FAK$^{\Delta myeloid}$ tibia appeared similar to those of littermate control animals.

As discussed above, Pyk2$^{-/-}$ mice exhibit an osteopetrotic phenotype marked by significantly greater BV/TV, Tb.Th, and Tb.N and significantly lower Tb.Sp than control animals [15]. The absence of an aberrant bone phenotype in FAK$^{\Delta myeloid}$ mice could be a result of the fact that Pyk2 compensates for a loss of FAK in these mice. Alternatively, it is possible that osteoclasts in these mice retain a critical threshold of FAK that is sufficient to maintain bone homeostasis. Indeed, low levels of FAK were detected routinely in osteoclasts derived from bone marrow progenitors isolated from FAK$^{\Delta myeloid}$ mice (for example, see Fig. 2A). To examine more directly the role of FAK in osteoclast function, the ability of WT and FAK-depleted osteoclasts to resorb bone was measured in vitro. WT and FAK-depleted Day 3 pOCs were plated on bone discs in the presence of M-CSF/RANKL, and the resorbed area was measured after 6 additional days of culture using ImageJ software (NIH). FAK-depleted cells underwent efficient osteoclast differentiation, fusion, and spreading, as determined by the percentage of TRAP+ cells and the size (area) of TRAP+ multinucleated cells (**Fig. 3A**). However, bone resorption by FAK-depleted osteoclasts was decreased by ~30% compared with WT cells (Fig. 3B). Thus, FAK is required for efficient bone resorption under these conditions. The fact that this functional deficiency is not manifest in the mouse may be a result of (1) incomplete loss of FAK in the osteoclast population present in the bone; (2) a greater complexity of factors within the bone microenvironment that regulate bone resorption compared with those present in the in vitro model used above; and/or (3) cellular and systemic factors in the animal that control the balance of bone degradation and bone formation.

FAK-depleted osteoclasts display reduced Erk activation but normal AKT activation upon M-CSF stimulation

Bone resorption by osteoclasts requires signaling networks that are initiated by ligand activation of integrin, cytokine, and CSF-1Rs [39]. In osteoclasts, Src and Pyk2 have been shown to function downstream of CSF-1R [13]. Signaling through FAK has not been studied in osteoclasts, but it has been shown to be an important effector of responses to M-CSF in macrophages [26]. To better understand the role of FAK in CSF-1R signaling networks in osteoclasts, AKT and Erk activation were measured in osteoclasts generated from WT and FAK$^{\Delta myeloid}$ mice following M-CSF stimulation. WT and FAK-depleted osteoclasts demonstrated a M-CSF-dependent activation of AKT

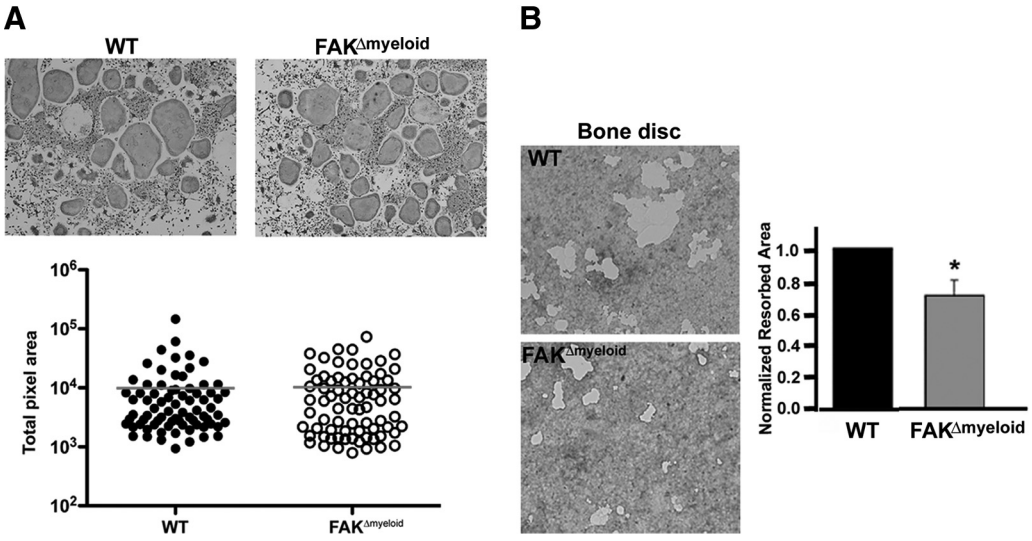

Figure 3. FAK-depleted results in impaired bone resorption in vitro. Bone marrow-differentiated WT and FAK-depleted pOCs were plated on bone discs in the presence of 10 ng/mL M-CSF and 50 ng/mL RANKL for 6 days. (A) TRAP-stained micrographs (4× original magnification) of fused, multinucleated WT and FAK$^{\Delta myeloid}$ osteoclasts (upper images). The area of 75 multinucleated cells was determined by tracing the perimeter of TRAP+ cells (greater than five nuclei) using ImageJ software (NIH; lower panel). (B) Resorption pit area was measured in three random fields and normalized to WT; $*P < 0.05$.

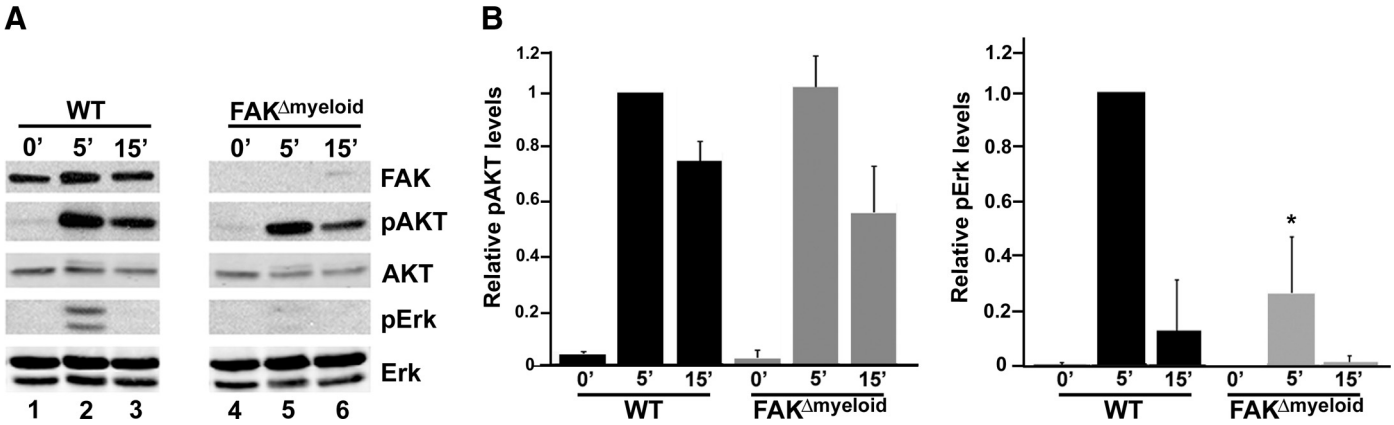

Figure 4. FAK is required for activation of Erk but not AKT downstream of M-CSF. Mature osteoclasts were starved of cytokines for 2 h and then stimulated with 30 ng/mL M-CSF for 5 and 15 min. (A) Lysate was collected, and representative immunoblots of three experiments measuring activation of Erk and AKT are shown. (B) Quantification of activation was performed by normalizing the phospho (p)-signal for each protein to total protein and then setting the maximal signal for each protein in WT cells (5 min) to 1; $n = 3$; $^*P < 0.05$ compared with WT.

that peaked at 5 min of stimulation (**Fig. 4**). Erk activation similarly peaked in WT cells at 5 min of M-CSF treatment but was more transient than AKT in that it returned to near-basal levels by 15 min. The FAK-depleted cells showed a significantly diminished Erk response at 5 min that returned back to basal levels by 15 min. This impaired Erk signaling may help to explain the reduced bone resorption exhibited by FAK-depleted cells, particularly in light of recent data showing that Erk plays a critical role in the process, whereby M-CSF enhances RANKL-induced osteoclast bone resorption [9].

Combined depletion of FAK and Pyk2 inhibits the differentiation of bone marrow precursors into large, multinucleated osteoclasts

As discussed above, osteoclasts are one of only a few cell types that express FAK and Pyk2. To determine the combined functions of FAK and Pyk2 in osteoclasts, the $FAK^{\Delta myeloid}$ mouse was crossed onto the genetic background of a global Pyk2 knockout [15, 24, 27] to produce a double-knockout in myeloid-lineage cells. Immunoblotting confirmed that FAK expression was decreased, and Pyk2 was absent in osteoclasts generated from these mice (**Fig. 5A**, lane 4; the residual FAK expression detected in these cells is likely a result of incomplete Cre-mediated recombination of the $FAK^{fl/fl}$ alleles). Whereas BV/TV was elevated significantly in mice harboring targeted deletion of FAK and Pyk2 compared with WT controls, it was not significantly different from that seen in $Pyk2^{-/-}$ mice (Supplemental Fig. 2). As we were unable to directly measure the efficiency of FAK depletion from osteoclasts in these mice, it was not possible to determine whether the similarity in bone phenotypes observed in $Pyk2^{-/-}$ and $FAK^{\Delta myeloid}/Pyk2^{-/-}$ animals was a result of the presence of residual FAK protein in the latter mice or the fact that Pyk2 but not FAK is essential for bone homeostasis.

To more fully understand the contributions of FAK and Pyk2 to osteoclast function, we turned to in vitro studies, as they allowed us to measure the efficiency of FAK depletion in each experiment. Following 6–7 days in M-CSF/RANKL, the majority of cells for all four genotypes was TRAP-positive, indicating that they were able to undergo differentiation (Fig. 5B). However, the size of the TRAP-positive, multinucleated cells appeared markedly reduced in cultures generated from the

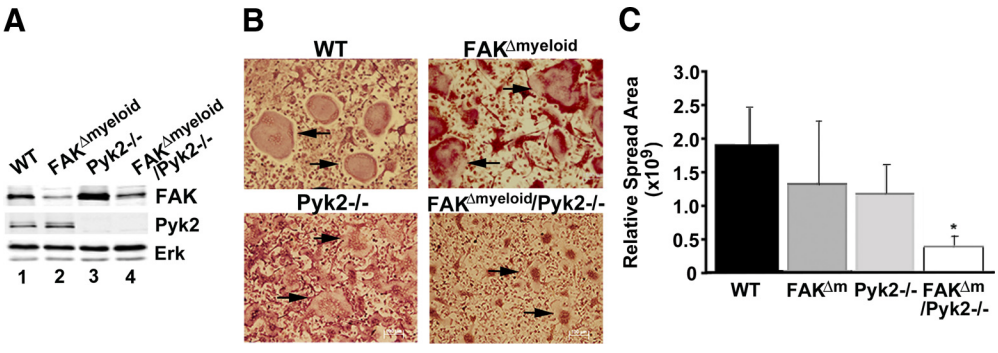

Figure 5. Combined depletion of FAK and loss of Pyk2 cause a decrease in the spread area of cultured osteoclasts. M-CSF-dependent bone marrow macrophages were differentiated into mature osteoclasts in the presence of M-CSF and RANKL for 6–7 days. (A) Lysate from mature osteoclasts derived from WT, $FAK^{\Delta myeloid}$, $Pyk2^{-/-}$, and $FAK^{\Delta myeloid}/Pyk2^{-/-}$ mice was separated by SDS-PAGE and immunoblotted for the designated antibodies. Immunoblots representative of four experiments are shown. (B) Cells cultured in this manner exhibited robust TRAP staining, indicative of mature osteoclasts. Arrows show examples of multinucleated cells. (C) The spread area of multinucleated cells was measured for three independent experiments (25 cells/experiment) using ImageJ software (NIH). Δm = Δmyeloid; $^*P < 0.05$ compared with WT.

FAK$^{\Delta myeloid}$/Pyk2$^{-/-}$ mice compared with those generated from WT, FAK$^{\Delta myeloid}$, or Pyk2$^{-/-}$ mice (Fig. 5B, arrows). This was confirmed by measuring the spread area of multinucleated cells in each of the cultures. Whereas FAK-depleted cells were highly variable in size, possibly as a result of variability in FAK levels, there was no statistically significant difference between the average spread area of these and WT cells (Fig. 5C). The same was the case for Pyk2$^{-/-}$ cells, in agreement with other reports showing that large, multinucleated osteoclasts can form in cells lacking Pyk2 [40]. In contrast, multinucleated cells from FAK$^{\Delta myeloid}$/Pyk2$^{-/-}$ mice were significantly smaller in size, indicating that at least one FAK family member is required for efficient cell fusion and/or spreading. However, either molecule alone is sufficient for these process(es), as large, multinucleated cells readily formed in cultures from both of the single knockout animals.

FAK and Pyk2 contribute to the organization of podosome structures

The marked defects in morphology exhibited by multinucleated osteoclasts derived from FAK$^{\Delta myeloid}$/Pyk2$^{-/-}$ mice prompted us to hypothesize that adhesion structures in the dual FAK/Pyk2$^{-/-}$ cells might be similarly impaired. Osteoclasts form podosomes at sites of contact with the ECM. Over time, these individual podosomes can then develop into higher-order clusters, rings, and belts that contribute to the establishment of sealing zones and efficient bone resorption [17, 21]. Pyk2$^{-/-}$ osteoclasts have been reported to form clusters and rings but are impaired in their ability to form complete belts [15]. To test the contribution of FAK to these processes, pOCs of all four genotypes were cultured on glass coverslips in the presence of M-CSF/RANKL for 6–7 days. The cells were then fixed, stained for actin and the podosome core protein cortactin, and processed for immunofluorescence microscopy. Under these conditions, WT and FAK-depleted cells exhibited the full array of podosome structures (individual podosomes, clusters/rings, and belts; **Fig. 6**). These data indicate that FAK is (1) not responsible for the establishment and/or maintenance of these structures; (2) the residual FAK present in the cells is sufficient to provide the requisite functions; or (3) Pyk2 effectively compensates for the absence of FAK. As has been reported previously [15], complete podosome belts were absent in Pyk2$^{-/-}$ osteoclasts (Fig. 6A, arrowheads), but podosome clusters and rings were present (Fig. 6B). However, the podosome structures in cells obtained from FAK$^{\Delta myeloid}$/Pyk2$^{-/-}$ mice were considerably more impaired than those present in Pyk2$^{-/-}$ cells. Single podosomes were the dominant structure in these cells (Fig. 6A, asterisk), whereas clusters/rings were extremely rare, and there was no evidence of podosome belts (Fig. 6B). These data show for the first time that, whereas Pyk2 appears to play an important role in regulating podosome dynamics in osteoclasts, FAK partially compensates for the absence of Pyk2 in Pyk2$^{-/-}$ cells. Interestingly, the podosome phenotype exhibited by cells derived from FAK$^{\Delta myeloid}$/Pyk2$^{-/-}$ mice is remarkably similar to that seen in cells generated from Src$^{-/-}$ mice [22]. Loss of Src in osteoclasts has been shown to disrupt podosome lifespan, actin flux, and podosome organization, resulting in fewer, more scattered podosome

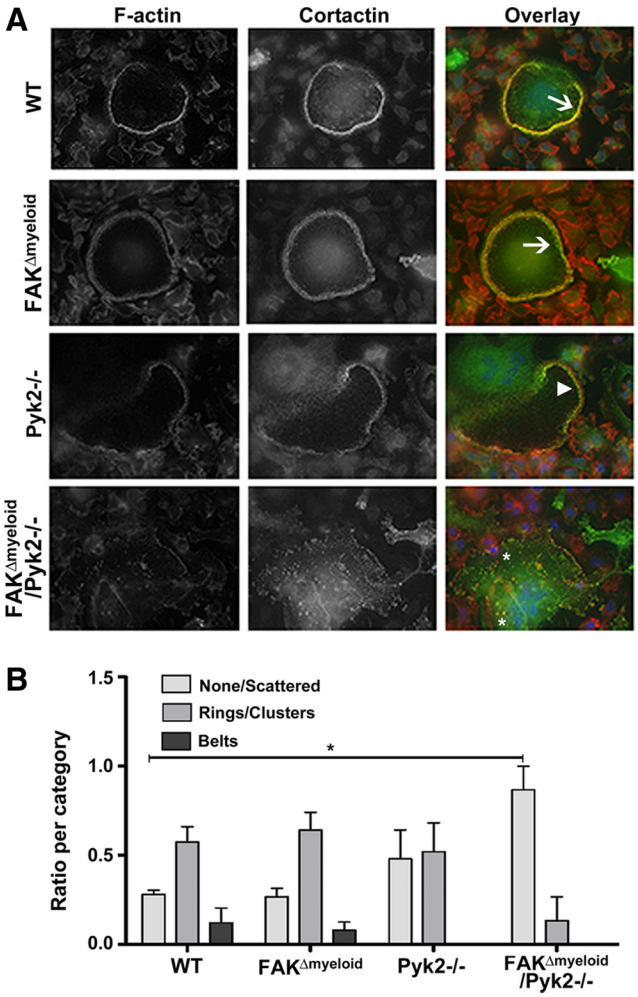

Figure 6. Podosome structures are disrupted significantly in the absence of FAK and Pyk2. Osteoclasts were fixed and stained for phalloidin (F-actin) and cortactin on Day 6 or 7. (A) Merged images are shown in the overlay with phalloidin (red), cortactin (green), and DAPI (blue; 40×). (B) Twenty-five cells containing 10–12 nuclei were evaluated/experiment for the presence of podosomes and were categorized as having none/scattered podosomes (light gray bars), clusters/rings (dark gray bars), or belts (black bars); $n = 3$; $^*P < 0.05$.

clusters and stunting the formation of rings and belts [22]. These similarities provide support for a potential coordination of function among FAK, Pyk2, and Src in the regulation of podosome organization and higher-order structure.

Conclusions

Skeletal homeostasis requires a balance between bone formation and bone degradation. Unchecked bone resorption by osteoclasts leads to bone that is porous, low-density, and subject to fracture. Understanding the molecular pathways that contribute to osteoclastic bone resorption is imperative for designing therapies to block osteoclast activity and detrimental bone loss. The purpose of the current study was to shed light on the relative contributions of FAK and its close relative Pyk2 to osteoclast function. Whereas Pyk2 was shown prior to these

studies to play an important role in osteoclast structure and activity, FAK function has been largely understudied in these cells. In this report, we show that FAK depletion in osteoclasts results in a 30% reduction in bone resorption in vitro. This functional deficiency does not appear to be a result of a failure of precursor cells to differentiate, fuse, spread, or form higher-order podosome structures, as osteoclast cultures isolated from bone marrow precursors of $FAK^{\Delta myeloid}$ mice appeared similar to those isolated from control littermates in each of these parameters. Instead, we suggest that the deficiency in bone-resorbing activity may be a result of a failure of osteoclasts to activate Erk effectively when FAK levels are reduced. Interestingly, AKT activation appears to occur through a distinct mechanism that does not require FAK, highlighting the fact that there are FAK-dependent and -independent M-CSF signaling networks in osteoclasts.

In contrast to the osteopetrotic phenotype exhibited by $Pyk2^{-/-}$ mice [15], $FAK^{\Delta myeloid}$ mice had no significant defect in BV or architecture. This could be a result of (1) a failure of $FAK^{\Delta myeloid}$ mice to reduce FAK expression in osteoclasts below a critical threshold necessary to maintain bone homeostasis; (2) the fact that Pyk2 may play a more dominant role than FAK in bone resorption by osteoclasts; and/or (3) the possibility that loss of Pyk2 in cells other than osteoclasts in the global $Pyk2^{-/-}$ mouse (e.g., osteoblasts) may contribute to the observed bone defect [40].

Finally, the $FAK^{\Delta myeloid}/Pyk2^{-/-}$ mouse that was generated for this study revealed novel information regarding the possible redundant functions of FAK and Pyk2 in osteoclast activities. Whereas incomplete FAK deletion made it difficult to assess phenotypes in vivo, decreased FAK expression in combination with a loss of Pyk2 had dramatic effects on osteoclast morphology and spreading that were significantly more pronounced than those seen under conditions of Pyk2 loss alone. The fact that these FAK-depleted/$Pyk2^{-/-}$ cells exhibited a similar phenotype to that reported for $Src^{-/-}$ osteoclasts suggests that all three PTKs may function in a coordinated manner to control osteoclast structure and function. Our finding that these kinases are also coordinately up-regulated during osteoclastogenesis strengthens this possibility.

AUTHORSHIP

B.J.R. performed all in vitro assays, contributed to experimental design and data analysis, and wrote the paper. K.T. assisted in in vitro assays. M.F.G. provided Supplemental Fig. 1. B.J.R. and C.S.H. performed in vivo bone scans and analyzed data. C.S.H. and E.A.B. provided microCT expertise. A.H.B. contributed to experimental design, data analysis, and wrote the paper.

ACKNOWLEDGMENTS

This work was supported by the U.S. National Institutes of Health (R21 CA135532 to A.H.B.; R01 DE019935 and R01 AR056445 to E.A.B.) and the Department of Defense (BC073291 to B.J.R.; BC093524 to M.F.G.; W81XWH1010928 to E.A.B.). This research was also supported by the University of Virginia Cancer Center through the Women's Oncology Research Fund, the Charlottesville Women's 4-Miler Breast Cancer Research Fund, and the National Cancer Institute Cancer Center Support Grant (P30 CA44579). We thank members of the laboratory and Drs. Thomas J. Parsons, Timothy Bender, Timothy Bullock, and Janet Cross for their input and expertise.

REFERENCES

1. Coleman, R. E. (2006) Clinical features of metastatic bone disease and risk of skeletal morbidity. *Clin. Cancer Res.* **12,** 6243s–6249s.
2. Saad, F., Lipton, A. (2010) SRC kinase inhibition: targeting bone metastases and tumor growth in prostate and breast cancer. *Cancer Treat. Rev.* **36,** 177–184.
3. Bagi, C. M., Roberts, G. W., Andresen, C. J. (2008) Dual focal adhesion kinase/Pyk2 inhibitor has positive effects on bone tumors: implications for bone metastases. *Cancer* **112,** 2313–2321.
4. Teitelbaum, S. L. (2000) Bone resorption by osteoclasts. *Science* **289,** 1504–1508.
5. Udagawa, N., Takahashi, N., Jimi, E., Matsuzaki, K., Tsurukai, T., Itoh, K., Nakagawa, N., Yasuda, H., Goto, M., Tsuda, E., Higashio, K., Gillespie, M. T., Martin, T. J., Suda, T. (1999) Osteoblasts/stromal cells stimulate osteoclast activation through expression of osteoclast differentiation factor/RANKL but not macrophage colony-stimulating factor: receptor activator of NF-κ B ligand. *Bone* **25,** 517–523.
6. Fuller, K., Owens, J. M., Jagger, C. J., Wilson, A., Moss, R., Chambers, T. J. (1993) Macrophage colony-stimulating factor stimulates survival and chemotactic behavior in isolated osteoclasts. *J. Exp. Med.* **178,** 1733–1744.
7. Jimi, E., Shuto, T., Koga, T. (1995) Macrophage colony-stimulating factor and interleukin-1 α maintain the survival of osteoclast-like cells. *Endocrinology* **136,** 808–811.
8. Suda, T., Tanaka, S., Takahashi, N. (1993) Macrophage colony-stimulating factor (M-CSF) is essential for differentiation rather than proliferation of osteoclast progenitors. *Osteoporos. Int.* **3** (Suppl. 1), 111–113.
9. Hodge, J. M., Collier, F. M., Pavlos, N. J., Kirkland, M. A., Nicholson, G. C. (2011) M-CSF potently augments RANKL-induced resorption activation in mature human osteoclasts. *PLoS One* **6,** e21462.
10. Insogna, K., Tanaka, S., Neff, L., Horne, W., Levy, J., Baron, R. (1997) Role of c-Src in cellular events associated with colony-stimulating factor-1-induced spreading in osteoclasts. *Mol. Reprod. Dev.* **46,** 104–108.
11. Nakamura, I., Lipfert, L., Rodan, G.A., Le, T. D. (2001) Convergence of α(v)β(3) integrin- and macrophage colony stimulating factor-mediated signals on phospholipase Cγ in prefusion osteoclasts. *J. Cell Biol.* **152,** 361–373.
12. Sanjay, A., Houghton, A., Neff, L., DiDomenico, E., Bardelay, C., Antoine, E., Levy, J., Gailit, J., Bowtell, D., Horne, W.C., Baron, R. (2001) Cbl associates with Pyk2 and Src to regulate Src kinase activity, α(v)β(3) integrin-mediated signaling, cell adhesion, and osteoclast motility. *J. Cell Biol.* **152,** 181–195.
13. Bruzzaniti, A., Neff, L., Sandoval, A., Du, L., Horne, W. C., Baron, R. (2009) Dynamin reduces Pyk2 Y402 phosphorylation and SRC binding in osteoclasts. *Mol. Cell. Biol.* **29,** 3644–3656.
14. Lowe, C., Yoneda, T., Boyce, B. F., Chen, H., Mundy, G. R., Soriano, P. (1993) Osteopetrosis in Src-deficient mice is due to an autonomous defect of osteoclasts. *Proc. Natl. Acad. Sci. USA* **90,** 4485–4489.
15. Gil-Henn, H., Destaing, O., Sims, N. A., Aoki, K., Alles, N., Neff, L., Sanjay, A., Bruzzaniti, A., De Camilli, P., Baron, R., Schlessinger, J. (2007) Defective microtubule-dependent podosome organization in osteoclasts leads to increased bone density in Pyk2(−/−) mice. *J. Cell Biol.* **178,** 1053–1064.
16. Sieg, D. J., Ilic, D., Jones, K. C., Damsky, C. H., Hunter, T., Schlaepfer, D. D. (1998) Pyk2 and Src-family protein-tyrosine kinases compensate for the loss of FAK in fibronectin-stimulated signaling events but Pyk2 does not fully function to enhance FAK− cell migration. *EMBO J.* **17,** 5933–5947.
17. Destaing, O., Saltel, F., Geminard, J. C., Jurdic, P., Bard, F. (2003) Podosomes display actin turnover and dynamic self-organization in osteoclasts expressing actin-green fluorescent protein. *Mol. Biol. Cell* **14,** 407–416.
18. Linder, S., Aepfelbacher, M. (2003) Podosomes: adhesion hot-spots of invasive cells. *Trends Cell Biol.* **13,** 376–385.
19. Tehrani, S., Faccio, R., Chandrasekar, I., Ross, F. P., Cooper, J. A. (2006) Cortactin has an essential and specific role in osteoclast actin assembly. *Mol. Biol. Cell* **17,** 2882–2895.
20. Luxenburg, C., Parsons, J. T., Addadi, L., Geiger, B. (2006) Involvement of the Src-cortactin pathway in podosome formation and turnover during polarization of cultured osteoclasts. *J. Cell Sci.* **119,** 4878–4888.

21. Luxenburg, C., Addadi, L., Geiger, B. (2006) The molecular dynamics of osteoclast adhesions. *Eur. J. Cell Biol.* **85,** 203–211.
22. Destaing, O., Sanjay, A., Itzstein, C., Horne, W. C., Toomre, D., De Camilli, P., Baron, R. (2008) The tyrosine kinase activity of c-Src regulates actin dynamics and organization of podosomes in osteoclasts. *Mol. Biol. Cell* **19,** 394–404.
23. Sasaki, H., Nagura, K., Ishino, M., Tobioka, H., Kotani, K., Sasaki, T. (1995) Cloning and characterization of cell adhesion kinase β, a novel protein-tyrosine kinase of the focal adhesion kinase subfamily. *J. Biol. Chem.* **270,** 21206–21219.
24. Okigaki, M., Davis, C., Falasca, M., Harroch, S., Felsenfeld, D. P., Sheetz, M. P., Schlessinger, J. (2003) Pyk2 regulates multiple signaling events crucial for macrophage morphology and migration. *Proc. Natl. Acad. Sci. USA* **100,** 10740–10745.
25. Schlaepfer, D. D., Hauck, C. R., Sieg, D. J. (1999) Signaling through focal adhesion kinase. *Prog. Biophys. Mol. Biol.* **71,** 435–478.
26. Owen, K. A., Pixley, F. J., Thomas, K. S., Vicente-Manzanares, M., Ray, B. J., Horwitz, A. F., Parsons, J. T., Beggs, H. E., Stanley, E. R., Bouton, A. H. (2007) Regulation of lamellipodial persistence, adhesion turnover, and motility in macrophages by focal adhesion kinase. *J. Cell Biol.* **179,** 1275–1287.
27. Yu, Y., Ross, S. A., Halseth, A. E., Hollenbach, P. W., Hill, R. J., Gulve, E. A., Bond, B. R. (2005) Role of PYK2 in the development of obesity and insulin resistance. *Biochem. Biophys. Res. Commun.* **334,** 1085–1091.
28. Fujikawa, Y., Quinn, J. M., Sabokbar, A., McGee, J. O., Athanasou, N. A. (1996) The human osteoclast precursor circulates in the monocyte fraction. *Endocrinology* **137,** 4058–4060.
29. Lin, T. H., Yurochko, A., Kornberg, L., Morris, J., Walker, J. J., Haskill, S., Juliano, R. L. (1994) The role of protein tyrosine phosphorylation in integrin-mediated gene induction in monocytes. *J. Cell Biol.* **126,** 1585–1593.
30. Kume, A., Nishiura, H., Suda, J., Suda, T. (1997) Focal adhesion kinase upregulated by granulocyte-macrophage colony-stimulating factor but not by interleukin-3 in differentiating myeloid cells. *Blood* **89,** 3434–3442.
31. Berry, V., Rathod, H., Pulman, L. B., Datta, H. K. (1994) Immunofluorescent evidence for the abundance of focal adhesion kinase in the human and avian osteoclasts and its down regulation by calcitonin. *J. Endocrinol.* **141,** R11–R15.
32. Duong, L. T., Lakkakorpi, P. T., Nakamura, I., Machwate, M., Nagy, R. M., Rodan, G. A. (1998) PYK2 in osteoclasts is an adhesion kinase, localized in the sealing zone, activated by ligation of α(v)β3 integrin, and phosphorylated by src kinase. *J. Clin. Invest.* **102,** 881–892.
33. Dodds, R. A., Connor, J. R., Drake, F., Feild, J., Gowen, M. (1998) Cathepsin K mRNA detection is restricted to osteoclasts during fetal mouse development. *J. Bone Miner. Res.* **13,** 673–682.
34. Horne, W. C., Neff, L., Chatterjee, D., Lomri, A., Levy, J. B., Baron, R. (1992) Osteoclasts express high levels of pp60c-src in association with intracellular membranes. *J. Cell Biol.* **119,** 1003–1013.
35. Cappellen, D., Luong-Nguyen, N. H., Bongiovanni, S., Grenet, O., Wanke, C., Susa, M. (2002) Transcriptional program of mouse osteoclast differentiation governed by the macrophage colony-stimulating factor and the ligand for the receptor activator of NFκ B. *J. Biol. Chem.* **277,** 21971–21982.
36. Park, M. H., Park, S. Y., Kim, Y. (2008) Induction of proline-rich tyrosine kinase2 (Pyk2) through C/EBPβ is involved in PMA-induced monocyte differentiation. *FEBS Lett.* **582,** 415–422.
37. Ilic, D., Furuta, Y., Kanazawa, S., Takeda, N., Sobue, K., Nakatsuji, N., Nomura, S., Fujimoto, J., Okada, M., Yamamoto, T. (1995) Reduced cell motility and enhanced focal adhesion contact formation in cells from FAK-deficient mice. *Nature* **377,** 539–544.
38. Clausen, B. E., Burkhardt, C., Reith, W., Renkawitz, R., Forster, I. (1999) Conditional gene targeting in macrophages and granulocytes using LysMcre mice. *Transgenic Res.* **8,** 265–277.
39. Novack, D.V., Faccio, R. (2011) Osteoclast motility: putting the brakes on bone resorption. *Ageing Res. Rev.* **10,** 54–61.
40. Buckbinder, L., Crawford, D. T., Qi, H., Ke, H. Z., Olson, L. M., Long, K. R., Bonnette, P. C., Baumann, A. P., Hambor, J. E., Grasser III, W. A., Pan, L. C., Owen, T. A., Luzzio, M. J., Hulford, C. A., Gebhard, D. F., Paralkar, V. M., Simmons, H. A., Kath, J. C., Roberts, W. G., Smock, S. L., Guzman-Perez, A., Brown, T. A., Li, M. (2007) Proline-rich tyrosine kinase 2 regulates osteoprogenitor cells and bone formation, and offers an anabolic treatment approach for osteoporosis. *Proc. Natl. Acad. Sci.* USA **104,** 10619–10624.

KEY WORDS:
Pyk2 · podosome · M-CSF